HHS Public Access

Author manuscript

Mol Cancer Res. Author manuscript; available in PMC 2020 August 01.

Published in final edited form as:

Mol Cancer Res. 2019 August ; 17(8): 1627–1638. doi:10.1158/1541-7786.MCR-18-1279.

BRD4 regulates metastatic potential of castration-resistant prostate cancer through AHNAK

Jordan S. Shafran[1,2], **Guillaume P. Andrieu**[1,3], **Balázs Győrffy**[4,5], **Gerald V. Denis**[1,2,6]

[1]Boston University-Boston Medical Center Cancer Center, Boston, Massachusetts, 02118, USA

[2]Department of Molecular and Translational Medicine, Boston University School of Medicine, Boston, Massachusetts, 02118, USA

[3]Current address: Institut Necker - Enfants Malades, Tour Pasteur - Étage 2, 75015 Paris, France

[4]MTA TTK Lendület Cancer Biomarker Research Group, Institute of Enzymology, 1117 Budapest, Hungary

[5]Semmelweis University, 2nd Department of Pediatrics, 1094 Budapest, Hungary

[6]Department of Pharmacology and Experimental Therapeutics, Boston University School of Medicine, Boston, Massachusetts, 02118, USA

Abstract

The inevitable progression of advanced prostate cancer to castration resistance, and ultimately to lethal metastatic disease, depends on primary or acquired resistance to conventional androgen-deprivation therapy (ADT) and accumulated resistance strategies to evade androgen receptor (AR) suppression. In prostate cancer cells, AR adaptations that arise in response to ADT are not singular, but diverse, and include gene amplification, mutation and even complete loss of receptor expression. Collectively, each of these AR adaptations contributes to a complex, heterogeneous, ADT-resistant tumor. Here, we examined prostate cancer cell lines that model common castration-resistant prostate cancer (CRPC) subtypes, each with different AR composition, and focused on novel regulators of tumor progression, the Bromodomain and ExtraTerminal (BET) family of proteins. We found that BRD4 regulates cell migration across all models of CRPC, regardless of aggressiveness and AR status, whereas BRD2 and BRD3 only regulate migration and invasion in less aggressive models that retain AR expression or signaling. BRD4, a co-regulator of gene transcription, controls migration and invasion through transcription of AHNAK, a large

Corresponding author: Gerald V. Denis, Boston University-Boston Medical Center Cancer Center, Rm K520, Boston University School of Medicine, 72 East Concord Street, Boston, Massachusetts, 02118, USA, Phone: 617-358-4785, Fax: 617-638-5673, gdenis@bu.edu.

Author Contributions

Conception and design: J.S. Shafran, G.P. Andrieu, G.V. Denis

Methodology: J.S. Shafran, G.P. Andrieu, G.V. Denis

Acquisition of data: J.S. Shafran

Analysis and interpretation of data: J.S. Shafran, G.P Andrieu, B. Győrffy, G.V. Denis

Writing, editing, and revision of manuscript: J.S. Shafran, G.P. Andrieu, B. Győrffy, G.V. Denis

Funding: G.V. Denis

Study supervision: G.V. Denis

Conflicts of interest: The authors state that they have no conflicts of interest to disclose.

Supplementary information: A file of supplementary figures and data is provided.

scaffolding protein linked to promotion of metastasis in a diverse set of cancers. Furthermore, treatment of CRPC cell lines with low doses of MZ1, a small-molecule, BRD4-selective degrader, inhibits metastatic potential. Overall, these results reveal a novel BRD4-AHNAK pathway that may be targetable to treat metastatic CRPC (mCRPC)

Keywords

bromodomain; prostate cancer; castration-resistant; epigenetic regulators; BET proteins; next-generation BET degrader; BRD4; AHNAK

INTRODUCTION

Prostate cancer is the second leading cause of cancer-related mortality in men in the United States (1). For patients who have recurrent prostate cancer or a disseminated form of the disease, the standard of care is androgen-deprivation therapy (ADT) (2). Despite an initial, nearly universal response that patients show to the anti-androgen drugs abiraterone, which inhibits the production of androgens, and enzalutamide, which prevents the androgen receptor (AR) from nuclear translocation and activation of AR-dependent genes (3), most patients invariably progress to castration-resistant prostate cancer (CRPC) and to a metastatic and incurable form of the disease (4,5). Prostate tumor cells acquire resistance to ADT through multiple mechanisms. These mechanisms, which are critical to cancer progression, include but are not limited to: aberrant androgen synthesis, AR gene amplifications, AR mutations, production of constitutively active AR splice variants and alternative steroid receptors (6–8). Whereas the majority of acquired mechanisms reactivate AR signaling and upregulate AR-dependent pro-metastatic and survival genes (9), recent data suggests that loss of AR expression due to sustained repression of AR signaling is an emerging mechanism of ADT resistance (10). Consistent with this finding, previous studies have demonstrated that some metastatic CRPC (mCRPC) tumors fail to express AR after ADT, or possibly even beforehand (11,12). Therefore, identification of novel, targetable mechanisms that critically regulate metastatic progression may offer valuable options to treat mCRPC, independent of aberrant AR signaling or alternative pathways that altogether bypass the androgen/AR axis.

Bromodomain and ExtraTerminal domain (BET) proteins (BRD2, BRD3, BRD4 and testis-specific BRDT) are a family of chromatin-associated proteins that regulate gene expression by acting as epigenetic readers through their ability to detect and bind to acetylated lysine residues on nucleosomal histone tails (13,14). Much effort has been invested in potential anti-cancer therapies that target BET proteins because of their roles as co-regulators of cell cycle progression (15) and cell proliferation (16). Consistent with this approach, small molecule pan-BET inhibitors such as JQ1 (17) and I-BET151 (18) have shown great promise as therapeutic agents across a diverse array of human malignancies (19,20), including CRPC (21,22). In cell line models of CRPC, JQ1 has been found to repress AR-V7 (an AR splice variant resistant to ADT (23)) expression (24) and AR-mediated gene transcription (25). More recently, ARV-771, a pan-BET degrader built on proteolysis-targeting chimera (PROTAC) technology, inhibited tumor growth in mouse models of CRPC (22). However,

even as pan-BET inhibitors and degraders become more widespread in their investigational and clinical use (26), accumulating evidence shows that pan-BET therapies can produce off-target effects, including the reactivation of latent HIV in infected T cells (27), and obscure the biology of each independently-acting BET protein (28). This caution underscores the need for more BET family member-selective chemical intervention (29).

Here, we investigate BET proteins as regulators of prostate cancer cell dissemination across multiple cell line models of CRPC. Notably, we show that BRD4, but not BRD2 or BRD3, regulates CRPC cell migration in all models. We identified AHNAK, a 700 kDa scaffolding protein that has been linked to migration and invasion in other aggressive cancers, as a BRD4-target gene to regulate CRPC cell migration and invasion. Survival analysis of prostate cancer cases with Cox proportional hazard models supports this interpretation. Furthermore, we provide evidence that the selective degradation of BRD4 with the innovative small molecule MZ1 (30) efficiently blocks CRPC metastatic potential. Overall, these results reveal a novel mechanism that could be targeted to treat mCRPC.

MATERIALS AND METHODS

Cell Culture

Human prostate cancer cell lines maintained at the NCI Office of Physical Sciences-Oncology Consortium (PS-OC), which supports a Network Bioresource Core Facility (PBCF) at the American Type Culture Collection, were contractually obtained through a Material Transfer Agreement. The cell lines had been authenticated by PBCF using karyotyping (Cell Line Genetics, Madison, WI), were tested in our facility for mycoplasma if infection was suspected, and passaged for fewer than six months. Experiments were conducted between passages three and six. The 22Rv1, DU 145 and PC-3 prostate cancer cell lines were cultured in RPMI-1640 medium (Gibco). VCaP prostate cancer cells were cultured in DMEM medium (Gibco). All culture media were supplemented with 10% fetal bovine serum (FBS, Corning) and 1% antibiotics (penicillin/streptomycin, Gibco). Cell lines were grown at 37°C in 5% CO_2. Mycoplasma contamination was prevented by treating cells with plasmocin (5 μg/mL for 2 weeks, Invivogen) after thawing and prior to experiments.

Antibodies and Reagents

The following antibodies were used: anti-BRD2, BRD3 and BRD4 (Bethyl Laboratories), anti-AR, anti-Flag and anti-β-Actin (Cell Signaling), anti-AHNAK (Abcam) and anti-α-tubulin (Santa Cruz Biotechnology). HRP-conjugated secondary antibodies were purchased from Bio-Rad. Fluorochrome-conjugated secondary antibodies were obtained from Jackson Laboratories. The active form of JQ1 ((+)-JQ1), the inactive form ((–)-JQ1) and MZ1 were purchased from Tocris.

Plasmids, siRNAs and Transfection

Lentivirus-mediated Flag-AHNAK expressing plasmid (EX-V0190-Lv242) and control vector (EX-NEG-Lv242) were purchased from GeneCopoeia. HEK-293 cells were co-transfected with plasmids encoding for VSV-G, dR8.2 dvpr and either Flag-AHNAK or control plasmid using Lipofectamine 2000 reagent (Thermo Fischer Scientific). Viral

supernatants were collected, and together with 4 μg/mL Polybrene (Millipore), were used to infect DU 145 cells for 48 hours. Stable clones were selected using medium containing 1 μg/mL puromycin (Invivogen). ON-Targetplus Human BET, Non-Targeting (scramble) and Human AHNAK SMARTpool siRNAs were purchased from Dharmacon. Cells were transfected with 25 nmol/L of listed siRNA for 72 hours with Lipofectamine 2000.

Immunoblot

Cell pellets were lysed in RIPA buffer (50 mmol/L Tris/HCl pH 7.5, 1 mmol/L EDTA, 0.5 mmol/L EGTA, 150 mmol/L NaCl, 0.1% sodium deoxycholate, 0.1% SDS, 1% Triton X-100). Samples containing 25 μg of protein were resolved by SDS-PAGE and transferred to nitrocellulose membranes. Membranes were saturated in TBS-BSA 5% to block non-specific binding sites, probed with primary antibodies and then visualized with HRP-conjugated secondary antibodies. Upon incubation in ECL, membranes were quantified with a gel imager.

qRT-PCR

Total RNA was extracted using the RNAeasy Kit (Qiagen). Reverse transcription reactions were performed with 1 μg of total RNA with the QuantiTect Reverse Transcription kit (Qiagen). The following genes were detected using the corresponding primers that were first checked for specificity with BLAST: *BRD2* (forward: 5'-CTACGTAAGAAACCCCGGAAG-3', reverse: 5'-GCTTTTTCTCCAAAGCCAGTT-3'), *BRD3* (forward: 5'-CCTCAGGGAGATGCTATCCA-3', reverse: 5'-ATGTCGTGGTAGTCGTGCAG-3'), *BRD4* (forward: 5'-TTTGAGACCCTGAAGCCGTC-3', reverse: 5'-TTAGGCAGGACCTGTTTCGG-3'), *AHNAK* (forward: 5'-GTGACCGAGATTCCCGACGA-3', reverse: 5'-AGCTCCCGGGTTGTCTCCTC-3'); the mean expression of the following housekeeping genes were used to normalize the results: *ACTB* (forward: 5'-ATTGGCAATGAGCGGTTCC-3', reverse: 5'-GGTAGTTTCGTGGATGCCACA-3'), *YWHAZ* (forward: 5'-ACTTTTGGTACATTGTGGCTTCAA-3', reverse: 5'-CCGCCAGGACAAACCAGTAT-3'). PCR amplifications were performed with MESA Green qPCR MasterMix (Eurogentec) on an ABI Prism 7500 thermal cycler.

Migration/invasion gene screening assay was performed using the RT^2 Profiler PCR EMT Array (Qiagen).

Chromatin Immunoprecipitation

DU 145 cells were treated with 400 nM of either (−)JQ1 or (+)JQ1 for 24 hours, fixed in 0.75% formaldehyde for 10 minutes, quenched with 125 mM glycine for 5 minutes and then lysed for chromatin immunoprecipitation (ChIP) as previously reported (31). Chromatin was precipitated with 1 μg anti-rabbit IgG (Cell Signaling) or anti-BRD4 (Bethyl Laboratories) with Protein A/G magnetic beads (Thermo Fisher Scientific). 5 ng of each sample was analyzed in triplicate by qPCR. The fold difference was calculated as 2^[Ct(input) - Ct(ChIP)], and fold enrichment over anti-IgG was assessed. ChIP primer sequences were as follows: *AHNAK* (forward: 5'-CCAGTAAACATGGGATACGAA-3', reverse: 5'-GAAGTGCTTTGCTCCACTCT-3').

Immunocytochemistry

Cells were fixed in absolute methanol for 5 minutes at - 20°C and then permeabilized with PBS, 0.2% Triton X-100 buffer for 10 minutes. After saturation in blocking buffer (0.02% Triton X-100, 2% BSA in PBS) for 30 minutes, permeabilized cells were incubated with primary antibodies and then fluorochrome-conjugated secondary antibodies (diluted in blocking buffer) for 1 hour. Lastly, coverslips were mounted with ProLong Gold with DAPI (Thermo Fischer Scientific). Image acquisition was conducted using a Leica DM IL LED inverted microscope. Fluorescence intensities were determined using ImageJ software (NIH). Intensities were measured from individual cells, corrected for background signal, and normalized by cell area.

Migration and Invasion Assays

JQ1: 22Rv1 and DU 145 cells were maintained in serum-free media + 400 nM of either active or inactive JQ1 for 3 hours prior to the beginning of experiments to suppress any basal migratory signals. VCaP cells were maintained in complete medium + 400 nM of either active or inactive JQ1 for 3 hours prior to the beginning of experiments. VCaP and 22Rv1 (225,000) or DU 145 (75,000) cells were seeded in Transwell inserts (pore size 8 μM, Corning) and challenged for migration. VCaP cells were exposed to FBS for 48 hours, 22Rv1 cells were exposed to 10% FBS for 24 hours, and DU 145 cells were exposed to 2.5% FBS for 6 hours.

siRNA: VCaP, 22Rv1 and DU 145 cells were seeded into Transwell inserts 72 hours after transfection using the conditions listed above. PC-3 cells (75,000) were maintained in serum-free media for 3 hours and then exposed to 10% FBS for 24 hours. For invasion assay, Matrigel (Corning) was diluted in serum-free media to a final concentration of 0.5 mg/mL and 100 μL was added onto the upper membranes prior to cell plating. Invasion was conducted for 16 hours using DU 145 cells using the corresponding conditions described above.

MZ1: 22Rv1 and DU 145 cells were treated with either 0.01% DMSO (control) or 10 nM (22Rv1) or 100 nM (DU 145) of MZ1 for 21 hours. Cells were then maintained in serum-free media with the aforementioned MZ1 concentration for 3 hours and then seeded into Transwell inserts using conditions listed above. VCaP cells were treated with either 0.01% DMSO or 10 nM MZ1 for 24 hours in complete medium and then seeded into Transwell inserts using corresponding conditions listed above. Invasion was conducted using the corresponding conditions described above.

Cells that did not migrate or invade were removed by wiping the upper side of the membrane with a cotton swab. Remaining cells were then fixed in absolute methanol for 5 minutes at −20°C. Cells were then stained with 1% crystal violet (Sigma) in 2% ethanol for 10 minutes. Images were captured using an EVOS XL Core digital inverted microscope. The percentage of migration and invasion was determined by first calculating the sum of the area of total migrated/invaded cells on the entire membrane by using ImageJ software, and then converted to relative percent migration/invasion by comparing each condition to the control condition (National Institutes of Health, Bethesda, Maryland).

MTT Cell Viability Assays

siRNA: VCaP, 22Rv1, DU 145 and PC-3 cells (15,000) were seeded in 96 well plates 24 hours (VCaP) or 48 hours (22Rv1, DU 145 and PC-3) after transfection.

MZ1: VCaP, 22Rv1 and DU 145 cells (15,000) cells were seeded in 96 well plates and then exposed to MZ1 at optimal BRD4-selective concentrations for 24 hours.

Post transfection (72 hours) or MZ1 treatment (24 hours), cells were then incubated with MTT (3-(4,5-dimethylthiazol-2-yl)-2,5-diphenyltetrazolium bromide) for 3 hours. Light absorbance was then measured at 570 nm and corrected for background absorbance at 690 nm with a multiwell spectrophotometer.

Kaplan-Meier and Clinical Parameter Analysis

To investigate the correlation between biochemical recurrence-free survival and *BRD4* and *AHNAK* expression, we utilized data from 421 patients from the TCGA repository. The normalized expression values of the RNAseq ID 23476 (for BRD4) and 79026 (for AHNAK) were used. For each gene, cutoff values were determined separately as described previously (32). Then, in order to assess the potential additive effects of the genes, samples with high BRD4 and high AHNAK were combined into one cohort, samples with low BRD4 and low AHNAK were combined into a second cohort, and all remaining patients with either high or low BRD4 and either high or low AHNAK were combined into a third cohort. Cox regression was used to compare the length of survival of the cohorts and a Kaplan-Meier plot was drawn to visualize the difference. As it is only possible to compute a hazard ratio (HR) for two groups, HR and p value are shown for biochemical recurrence-free survival by comparing the $BRD4^{high}$ and $AHNAK^{high}$ and the $BRD4^{low}$ and $AHNAK^{low}$ cohorts. To exclude BRD4 or AHNAK mutation bias, we determined that less than 1% of the 421 patients profiled had mutations in either BRD4 or AHNAK (data not shown).

We compared the expression of both genes to Gleason score, pathological T and N status. Sample number with a positive event for pathological M was too low for meaningful analysis. Expression values were compared by a Kruskal-Wallis H-test (Gleason and T pathological) and Mann-Whitney T-test (N pathological). Finally, we used the patient samples to directly compare BRD4 and AHNAK expressions by drawing a linear regression and computing a Spearman rank correlation. The gene expression data with clinical annotation including pathological TNM, Gleason score and survival times are listed in Supplementary Tables S1 and S2.

Statistical Analysis

Statistical analyses of the *in vitro* experiments were performed using Student's t test or ANOVA as indicated, and were generated by GraphPad Prism software. $p < 0.05$ was considered statistically significant.

RESULTS

Pan-BET inhibition reduces prostate cancer cell migration in multiple models of CRPC

CRPC is an advanced and aggressive form of prostate cancer associated with poor survival outcomes (33). Genomic analyses of mCRPC tumors from patients who have undergone ADT reveal that AR is heterogeneous in both status (over 60% of profiled tumors have either a mutation or amplification of AR (34,35)) and expression (over 20% of profiled tumors fail to express AR (10)). To determine whether BET proteins regulate CRPC cell migration, we used different cell line models that capture some of the AR heterogeneity of CRPC (VCaP: AR-Wild-type/Amplified (WT/Amp); 22Rv1: AR-mutant (H874Y) and DU 145: AR-null (36,37) (Fig. 1A). Our approach was first to use the pan-BET inhibitor JQ1, a small molecule that displaces BRD2, BRD3 and BRD4 from chromatin (17), to evaluate its effect on prostate cancer cell migration. VCaP, 22Rv1 and DU 145 cells were pretreated with either the active (+) form or inactive (−) form of JQ1 for 3 hours, and then challenged for migration using a transwell system. (+)JQ1 reduced migration of VCaP, 22Rv1 and DU 145 cells by 85%, 57% and 28% respectively (Fig. 1B, C and D). Taken together, these data indicate that BET protein functions are essential for CRPC cell migration.

BRD4 regulates CRPC cell migration irrespective of AR status

Upon confirming that BET proteins are critical for CRPC cell migration, we determined whether each BET protein is needed for migration in each model. JQ1 is not a BET isoform-selective inhibitor (17), thus we used a BET-specific siRNA knockdown approach to target each BET protein individually. Transfection of VCaP, 22Rv1 and DU 145 cells with control scramble siRNA or BET-specific siRNAs selectively ablated the mRNA (Supplementary Fig. S1A–D) and protein of each BET gene (Fig. 2A, D and G). Cell viability was assessed by MTT assay under the aforementioned transfection conditions to ensure that any ensuing migratory effect was a result of BET protein depletion and not due to cell death. Viability of control and BET depleted VCaP, 22Rv1 and DU 145 cells was comparable across all conditions (Fig. 2B, E and H). We next measured the migratory capacity of BET protein-depleted cells in each model with the Transwell system. Individual depletion of either BRD2, BRD3 or BRD4 significantly reduced migration in VCaP cells (Fig. 2C), matching an invasive phenotype previously reported (25). Depletion of either BRD2 or BRD4 in 22Rv1 cells reduced migration by 53%, whereas knockdown of BRD3 had no effect on migration (Fig. 2F). Interestingly, whereas migration in VCaP and 22Rv1 cells was regulated by more than one BET protein, the knockdown of only BRD4 - and not of BRD2 or BRD3 - significantly reduced DU 145 cell migration (Fig. 2I). The same phenotype was also observed when measuring invasion (Supplementary Fig. S2A). Furthermore, a similar BRD4-dependent migration phenotype was also observed in PC-3 cells (highly metastatic, AR-null) (Supplementary Fig. S2B–D). Remarkably though, depletion of BRD2 opposed the effect of BRD4 in this model, and increased migration by 48% (Supplementary Fig. S2B–D). Collectively, these results identify BRD4, and not BRD2 or BRD3, as the dominant regulator of CRPC cell migration and invasion, and also illustrates the complex, non-overlapping and even opposing functions that BET proteins can have in their regulation of a particular biological process.

Discovery of *AHNAK* as a BRD4 target gene

In order to identify BRD4 target genes that mediate CRPC cell dissemination, we carried out a gene expression analysis in control and BET protein-depleted DU 145 cells. We curated a panel of 73 genes that we previously showed were involved in pathways important for cell migration, invasion and metastasis (31). Depletion of BRD4 by siRNA knockdown produced a significant change in the expression of three genes when compared to BRD2 and BRD3 depleted cells (two upregulated, one downregulated, Z score ≥ 2 or ≤ −2, Fig. 3A). Of the three differentially expressed genes, only *AHNAK*, a 700 kDa scaffolding protein was downregulated (38). Known primarily for its ability to facilitate the formation of multi-protein complexes (39,40), AHNAK more recently has been shown to be important for the development of pseudopodial protrusions and tumor cell migration and invasion (41,42). Therefore, we considered that this potential target gene had important translational significance worth deeper investigation. To verify our findings that *AHNAK* is a BRD4 target gene, we first measured AHNAK mRNA and protein expression in each of our models upon BET protein depletion. Indeed, knockdown of BRD4, and not of BRD2 or BRD3 dramatically downregulated both AHNAK mRNA and protein expression (Fig. 3B–G; Supplementary Fig. S3A and S3B). We then assessed if BRD4 associates with the AHNAK promoter by ChIP (43). We found that BRD4 interacts with the AHNAK promoter, and that treatment with (+)JQ1 disrupts this interaction (Supplementary Fig. S3C). These results confirm that *AHNAK* is a BRD4 target gene, and that this relationship is conserved even in the absence of AR expression.

BRD4-AHNAK signaling pathway regulates CRPC cell migration

AHNAK promotes tumor metastasis and has previously been shown to regulate migration and invasion in DU 145 cells (41,44). We therefore hypothesized that AHNAK is critical for CRPC cell migration and invasion. To test this hypothesis, we first validated siRNA against *AHNAK* in each of our models (Fig. 4A, B, E, F, I and J). Upon confirming depletion of *AHNAK* in each model, we then measured its effect on migration. Notably, knockdown of *AHNAK* by siRNA reduced migration in VCaP, 22Rv1 and DU 145 cells by 38%, 43% and 33% respectively (Fig. 4C, G and K). Likewise, AHNAK-depleted DU 145 cells had invasion reduced by 26% (Supplementary Fig. S4A). Based on these results, we predicted that BRD4 acts upstream from AHNAK and regulates prostate cancer cell migration and invasion through a BRD4-AHNAK signaling pathway. We would then expect that the co-depletion of BRD4 and AHNAK would not further reduce migration. As expected, the co-depletion of BRD4 and AHNAK reduced migration in all models to levels comparable to depletion of either BRD4 or AHNAK alone (Fig. 4D, H and L). Furthermore, if BRD4 acts upstream of AHNAK, AHNAK overexpression in BRD4-depleted cells should rescue cell migration. To test this hypothesis, we overexpressed AHNAK in DU 145 cells (Supplementary Fig. S4B and S4C) using a Flag-AHNAK plasmid (45,46). We found that overexpression of AHNAK increased migration in DU 145 cells by 23% in siRNA control cells (Supplementary Fig. S4D). Significantly, overexpression of AHNAK rescued cell migration in BRD4-depleted cells (Supplementary Fig. S4D). Together, these results identify *AHNAK* as a BRD4 target gene that regulates CRPC cell migration and invasion.

Selective degradation of BRD4 inhibits CRPC cell migration

BET proteins can have individual, non-overlapping roles (28). JQ1 and BET degraders like ARV-771 lack intra-BET selectivity and leave open the possibility of off-target effects in a therapeutic setting (17,22,27). Therefore, we tested whether MZ1, a novel small molecule BET degrader built on Proteolysis Targeted Chimeras (PROTAC) technology that has been shown to be BRD4 selective at low doses (30), could selectively degrade BRD4 and inhibit migration and invasion in our CRPC models. In control experiments, we confirmed that treatment of VCaP, 22Rv1 and DU 145 cells with low doses of MZ1 for 24 hours preferentially degraded BRD4 over BRD2 and BRD3 in all models (Fig. 5A, D and G) without affecting cell viability (Supplementary Fig. S5A–C). Furthermore, degradation of BRD4 by MZ1 reduced the expression of AHNAK and inhibited CRPC cell migration and invasion to comparable levels produced by siRNA against BRD4 (Fig. 5B, C, E, F, H and I; Supplementary Fig. S5D). These results show that BRD4 can be selectively degraded in models of CRPC that differ greatly by aggressiveness and heterogeneity. This degradation effectively inhibits metastatic potential.

BRD4 and AHNAK expression associate with prostate cancer clinical parameters and biochemical recurrence-free survival

Prostate cancer clinical parameters, a collection of measurements that determine tumor aggressiveness (Gleason Score) and stage (Tumor-Node-Metastasis), have been shown to associate with high biochemical-recurrence (BCR) rates, and together, are significant predicators of metastatic disease progression (47). Furthermore, BRD4 expression has been shown to associate with prostate cancer patient outcomes and increase with castration resistance (48,49). Therefore, we tested the hypothesis that BRD4 and AHNAK are critical to the clinical progression of CRPC, and determined whether *BRD4* and *AHNAK* expression correlate with prostate cancer clinical parameters and BCR-free survival. When comparing the expression of BRD4 to prostate cancer clinical parameters, there was a significant correlation *in vivo* to Gleason score ($p = 0.0089$, Fig. 6A), pathological T ($p = 0.028$, Fig. 6B) and pathological N ($p = 0.0018$, Fig. 6C). Interestingly, no significant correlation between these parameters and AHNAK expression was observed (data not shown). However, when comparing BRD4 and AHNAK expression, there was a significant correlation between the two genes ($p = 1.5e\text{-}14$, correlation coefficient = 0.33, Fig. 6D). Furthermore, data from a smaller 2015 study that performed whole exome sequencing from 150 mCRPC patients show a borderline significant correlation between BRD4 and AHNAK expression (Supplementary Fig. S6) (35,50,51). Lastly, we performed a meta-analysis of 421 patients with adenocarcinoma of the prostate using the TCGA repository, and determined that *BRD4* and *AHNAK* expression correlate with BCR-free survival. High expression of *BRD4* and *AHNAK* were significantly associated with a shorter time to BCR in prostate cancer patients (Fig. 6E; HR = 2.38, log-rank $p = 0.013$). In summary, expression of BRD4 and AHNAK significantly influences clinical and pathological characteristics associated with metastatic disease progression in prostate cancer patients.

Discussion

Our work establishes that among the BET protein family, BRD4, but not BRD2 or BRD3, is the principal regulator of CRPC cell migration and invasion. Treatment of CRPC cells with JQ1, a pan-BET inhibitor, left open the possibility that each of BRD2, BRD3 and BRD4 were responsible for regulating CRPC cell migration in all models (Fig. 1). Although previous studies have suggested that each BET family member is critical in mediating metastatic properties in cell line models of CRPC (22,24), we used BET-selective siRNAs to prove that BRD4 alone is essential. We also provide evidence that suggests that the functional requirement for BET family members depends on AR status. BRD4 regulated cell migration across all models of CRPC, regardless of aggressiveness and AR status, whereas BRD2 and BRD3 only regulated migration in less aggressive models that retained AR expression or signaling (Fig. 2). These findings demonstrate once again that for a common biological function, each BET family member is capable of exerting its own independent function, while at the same time individual BET proteins are also capable of generating overlapping or even opposing effects (Supplementary Fig. S2B–D) (28).

Because only BRD4 consistently regulated pro-metastatic properties in each of our models, we hypothesized that a common set of BRD4 target gene(s) exists, and that these target genes are critical for migration and invasion. In that pursuit, we identified AHNAK, a large scaffolding protein previously shown to contribute to cell migration and invasion in prostate cancer cells (41), as a BRD4 target gene in DU 145 cells (Fig. 3A). We then determined whether the BRD4-AHNAK relationship was unique to AR-null CRPC cell models (Fig. 3F and G; Supplementary Fig. S3A and S3B), or conserved across all CRPC models. A previous report showed that upon loss of AR, signaling networks that were prominent in AR-competent cells failed to play the same role in cells that were no longer dependent on AR-mediated transcription (10). Intriguingly, we discovered that AHNAK was a BRD4 target gene in all models (Fig. 3B–E), evidenced by BRD4 interaction with AHNAK promoter chromatin (Supplementary Fig. S3C), suggesting that this newly identified BRD4-AHNAK relationship is conserved regardless of AR status. This result stands apart to previous reports that BET family members directly interact with and regulate a set of AR target genes (25). AR signaling is known to control prostate cancer cell migration and invasion (52). Thus, it is likely that BET proteins regulate prostate cancer cell migration and invasion *via* at least two co-existing mechanisms: through AR signaling and through AHNAK. In AR signaling-proficient cells, BET proteins bind to AR and drive expression of several AR-dependent genes (25), including pro-metastatic genes. We have shown that the BRD4/AHNAK axis regulates migration and invasion in our models regardless of AR status. Therefore, BRD4 targeting would alter these two pathways concomitantly and dramatically impair cell dissemination. However, in AR-deficient cells, the subsequent AR-dependent BET-mediated pathways driving migration and invasion are lost, thus the BRD4/AHNAK axis may become predominant. Because AHNAK was regulated by BRD4 in all models, it allowed us to determine its significance in cell migration and invasion. Consistent with this model, AHNAK was found to play a critical role in mediating cell migration and invasion in our models (Fig. 4; Supplementary Fig. S4A–D), reinforcing newly published results that establish AHNAK as a critical mediator of tumor metastasis (44). In addition to its

contribution to the development of pseudopodia (41), other reports have shown that AHNAK plays an integral role in both SMAD3 and RAF-MEK-ERK signaling, as an intermediary for these canonical signaling pathways (44,53). Based on these previous findings, we hypothesize that AHNAK serves dual roles in its regulation of CRPC cell dissemination. We suspect that it functions as a key structural component in the formation of pseudopodia which allows prostate cancer cells to protrude and induce invasive/migratory behavior, while also serving as a downstream effector for key signaling pathways that relay critical signals (i.e. chemokines and cytokines) from the tumor microenvironment. Each of these potential functions illustrates AHNAK's significance to the larger process of CRPC dissemination and metastasis, and thus it is not surprising that the expression of both AHNAK and BRD4 correlate with critical prostate cancer clinical markers and BCR-free survival in prostate cancer patients (Fig. 6; Supplementary Fig. S6).

Treatment for patients with CRPC always includes a means to disrupt the androgen/AR axis, and while effective for an average of 2–3 years, ADT inevitably fails to impede progression due to the acquired resistance mechanisms that come as a result of AR adaptations (4). Because of this understanding, new therapies that go beyond directly targeting the AR to treat CRPC have begun to emerge, including a multitude of pan-BET inhibitors and degraders (22,54–56). Although each of these new therapeutics have been shown successfully to inhibit or degrade the BET family of proteins, they lack intra-BET selectivity and have primarily been shown to regulate cell proliferation and viability only in models of CRPC that retain AR expression. These results are misleading because they give the false impression that targeting BET proteins is only viable in AR-competent models of CRPC, yet the data outlined throughout this report show that BRD4 retains functionality to regulate pro-metastatic properties in models of CRPC that are both AR-competent and AR-deficient. As we and others have reported previously, the need for pan-BET inhibition or degradation is context and cancer dependent. BET proteins are not always functionally redundant, and because each family member regulates transcription in a unique way, investigators must first elucidate the relevant BET proteins for any specific biological function. Based on that principle, and the findings reported here in Fig 2–4, we selectively targeted BRD4 in each of our models using low doses of MZ1 (10–100 nM), and achieved similar migration and invasion results obtained using siRNA against BRD4 (Fig. 5; Supplementary Fig. S5D). MZ1 is a Proteolysis Targeted Chimeras (PROTAC) degrader, and has been shown to preferentially degrade BRD4 over BRD2 and BRD3 in certain cell lines (30). Whereas other PROTAC molecules like ARV-771 and dBET1/dBET2 appear to not discriminate among the BET family of proteins (22,54), crystallographic and biophysical studies have shown that the specific nature of the ternary complex formed by MZ1 with the E3 ligase VHL and the BRD4 bromodomain defines this BRD4 selectivity (57). Future studies will need to validate MZ1's efficacy and selectivity in more advanced model systems, yet the work shown here (Fig. 7) provides a novel mechanism that could be targeted with therapies like MZ1 or related BRD4-selective degraders to treat patients with mCRPC.

Supplementary Material

Refer to Web version on PubMed Central for supplementary material.

Acknowledgements

We thank Dr. Alessio Ciulli for providing MZ1 and helpful discussion. We also thank Drs. Gretchen Gignac and Ariel Hirsch for insightful comments and helpful discussion, Dr. Nader Rahimi for providing HEK293 cells and Dr. Naser Jafari for providing plasmids that encode VSV-G and dR8.2 dvpr. J. Shafran is supported by a T32 training grant, 'Research Training in Immunology' from NIAID (5T32AI007309–30, PI Kepler). The funders had no role in study design, data collection and analysis, decision to publish, or preparation of the manuscript.

Grant support: This study was supported by grants from the National Institutes of Health (DK090455, U01CA182898, R01CA222170; GV Denis; T32AI007309; TB Kepler).

References

1. Siegel RL, Miller KD, Jemal A. Cancer statistics, 2018. CA Cancer J Clin 2018;68(1):7–30 doi 10.3322/caac.21442. [PubMed: 29313949]
2. Connolly RM, Carducci MA, Antonarakis ES. Use of androgen deprivation therapy in prostate cancer: indications and prevalence. Asian J Androl 2012;14(2):177–86 doi 10.1038/aja.2011.103. [PubMed: 22231299]
3. Paller CJ, Antonarakis ES. Management of biochemically recurrent prostate cancer after local therapy: evolving standards of care and new directions. Clin Adv Hematol Oncol 2013;11(1):14–23. [PubMed: 23416859]
4. Karantanos T, Corn PG, Thompson TC. Prostate cancer progression after androgen deprivation therapy: mechanisms of castrate resistance and novel therapeutic approaches. Oncogene 2013;32(49):5501–11 doi 10.1038/onc.2013.206. [PubMed: 23752182]
5. Hotte SJ, Saad F. Current management of castrate-resistant prostate cancer. Curr Oncol 2010;17 Suppl 2:S72–9. [PubMed: 20882137]
6. Watson PA, Arora VK, Sawyers CL. Emerging mechanisms of resistance to androgen receptor inhibitors in prostate cancer. Nat Rev Cancer 2015;15(12):701–11 doi 10.1038/nrc4016. [PubMed: 26563462]
7. Chandrasekar T, Yang JC, Gao AC, Evans CP. Mechanisms of resistance in castration-resistant prostate cancer (CRPC). Transl Androl Urol 2015;4(3):365–80 doi 10.3978/j.issn. 2223-4683.2015.05.02. [PubMed: 26814148]
8. Cattrini C, Zanardi E, Vallome G, Cavo A, Cerbone L, Di Meglio A, et al. Targeting androgen-independent pathways: new chances for patients with prostate cancer? Crit Rev Oncol Hematol 2017;118:42–53 doi 10.1016/j.critrevonc.2017.08.009. [PubMed: 28917268]
9. Hoang DT, Iczkowski KA, Kilari D, See W, Nevalainen MT. Androgen receptor-dependent and -independent mechanisms driving prostate cancer progression: Opportunities for therapeutic targeting from multiple angles. Oncotarget 2017;8(2):3724–45 doi 10.18632/oncotarget.12554. [PubMed: 27741508]
10. Bluemn EG, Coleman IM, Lucas JM, Coleman RT, Hernandez-Lopez S, Tharakan R, et al. Androgen Receptor Pathway-Independent Prostate Cancer Is Sustained through FGF Signaling. Cancer Cell 2017;32(4):474–89 e6 doi 10.1016/j.ccell.2017.09.003. [PubMed: 29017058]
11. Roudier MP, True LD, Higano CS, Vesselle H, Ellis W, Lange P, et al. Phenotypic heterogeneity of end-stage prostate carcinoma metastatic to bone. Hum Pathol 2003;34(7):646–53. [PubMed: 12874759]
12. Shah RB, Mehra R, Chinnaiyan AM, Shen R, Ghosh D, Zhou M, et al. Androgen-independent prostate cancer is a heterogeneous group of diseases: lessons from a rapid autopsy program. Cancer Res 2004;64(24):9209–16 doi 10.1158/0008-5472.CAN-04-2442. [PubMed: 15604294]
13. Denis GV, Green MR. A novel, mitogen-activated nuclear kinase is related to a Drosophila developmental regulator. Genes Dev 1996;10(3):261–71. [PubMed: 8595877]
14. Belkina AC, Blanton WP, Nikolajczyk BS, Denis GV. The double bromodomain protein Brd2 promotes B cell expansion and mitogenesis. J Leukoc Biol 2014;95(3):451–60 doi 10.1189/jlb. 1112588. [PubMed: 24319289]

15. Dey A, Chitsaz F, Abbasi A, Misteli T, Ozato K. The double bromodomain protein Brd4 binds to acetylated chromatin during interphase and mitosis. Proc Natl Acad Sci U S A 2003;100(15): 8758–63 doi 10.1073/pnas.1433065100. [PubMed: 12840145]

16. Denis GV, Vaziri C, Guo N, Faller DV. RING3 kinase transactivates promoters of cell cycle regulatory genes through E2F. Cell Growth Differ 2000;11(8):417–24. [PubMed: 10965846]

17. Filippakopoulos P, Qi J, Picaud S, Shen Y, Smith WB, Fedorov O, et al. Selective inhibition of BET bromodomains. Nature 2010;468(7327):1067–73 doi 10.1038/nature09504. [PubMed: 20871596]

18. Dawson MA, Prinjha RK, Dittmann A, Giotopoulos G, Bantscheff M, Chan WI, et al. Inhibition of BET recruitment to chromatin as an effective treatment for MLL-fusion leukaemia. Nature 2011;478(7370):529–33 doi 10.1038/nature10509. [PubMed: 21964340]

19. Garcia PL, Miller AL, Kreitzburg KM, Council LN, Gamblin TL, Christein JD, et al. The BET bromodomain inhibitor JQ1 suppresses growth of pancreatic ductal adenocarcinoma in patient-derived xenograft models. Oncogene 2016;35(7):833–45 doi 10.1038/onc.2015.126. [PubMed: 25961927]

20. Gao Z, Yuan T, Zhou X, Ni P, Sun G, Li P, et al. Targeting BRD4 proteins suppresses the growth of NSCLC through downregulation of eIF4E expression. Cancer Biol Ther 2018;19(5):407–15 doi 10.1080/15384047.2018.1423923. [PubMed: 29333921]

21. Wyce A, Degenhardt Y, Bai Y, Le B, Korenchuk S, Crouthame MC, et al. Inhibition of BET bromodomain proteins as a therapeutic approach in prostate cancer. Oncotarget 2013;4(12):2419–29 doi 10.18632/oncotarget.1572. [PubMed: 24293458]

22. Raina K, Lu J, Qian Y, Altieri M, Gordon D, Rossi AM, et al. PROTAC-induced BET protein degradation as a therapy for castration-resistant prostate cancer. Proc Natl Acad Sci U S A 2016;113(26):7124–9 doi 10.1073/pnas.1521738113. [PubMed: 27274052]

23. Antonarakis ES, Lu C, Wang H, Luber B, Nakazawa M, Roeser JC, et al. AR-V7 and resistance to enzalutamide and abiraterone in prostate cancer. N Engl J Med 2014;371(11):1028–38 doi 10.1056/NEJMoa1315815. [PubMed: 25184630]

24. Asangani IA, Wilder-Romans K, Dommeti VL, Krishnamurthy PM, Apel IJ, Escara-Wilke J, et al. BET Bromodomain Inhibitors Enhance Efficacy and Disrupt Resistance to AR Antagonists in the Treatment of Prostate Cancer. Mol Cancer Res 2016;14(4):324–31 doi 10.1158/1541-7786.MCR-15-0472. [PubMed: 26792867]

25. Asangani IA, Dommeti VL, Wang X, Malik R, Cieslik M, Yang R, et al. Therapeutic targeting of BET bromodomain proteins in castration-resistant prostate cancer. Nature 2014;510(7504):278–82 doi 10.1038/nature13229. [PubMed: 24759320]

26. Doroshow DB, Eder JP, LoRusso PM. BET inhibitors: a novel epigenetic approach. Ann Oncol 2017;28(8):1776–87 doi 10.1093/annonc/mdx157. [PubMed: 28838216]

27. Banerjee C, Archin N, Michaels D, Belkina AC, Denis GV, Bradner J, et al. BET bromodomain inhibition as a novel strategy for reactivation of HIV-1. J Leukoc Biol 2012;92(6):1147–54 doi 10.1189/jlb.0312165. [PubMed: 22802445]

28. Andrieu GP, Denis GV. BET Proteins Exhibit Transcriptional and Functional Opposition in the Epithelial-to-Mesenchymal Transition. Mol Cancer Res 2018;16(4):580–6 doi 10.1158/1541-7786.MCR-17-0568. [PubMed: 29437854]

29. Baud MGJ, Lin-Shiao E, Cardote T, Tallant C, Pschibul A, Chan KH, et al. Chemical biology. A bump-and-hole approach to engineer controlled selectivity of BET bromodomain chemical probes. Science 2014;346(6209):638–41 doi 10.1126/science.1249830. [PubMed: 25323695]

30. Zengerle M, Chan KH, Ciulli A. Selective Small Molecule Induced Degradation of the BET Bromodomain Protein BRD4. ACS Chem Biol 2015;10(8):1770–7 doi 10.1021/acschembio.5b00216. [PubMed: 26035625]

31. Andrieu G, Tran AH, Strissel KJ, Denis GV. BRD4 Regulates Breast Cancer Dissemination through Jagged1/Notch1 Signaling. Cancer Res 2016;76(22):6555–67 doi 10.1158/0008-5472.CAN-16-0559. [PubMed: 27651315]

32. Budczies J, Klauschen F, Sinn BV, Gyorffy B, Schmitt WD, Darb-Esfahani S, et al. Cutoff Finder: a comprehensive and straightforward Web application enabling rapid biomarker cutoff

optimization. PLoS One 2012;7(12):e51862 doi 10.1371/journal.pone.0051862. [PubMed: 23251644]

33. Kirby M, Hirst C, Crawford ED. Characterising the castration-resistant prostate cancer population: a systematic review. Int J Clin Pract 2011;65(11):1180–92 doi 10.1111/j.1742-1241.2011.02799.x. [PubMed: 21995694]
34. Beltran H, Yelensky R, Frampton GM, Park K, Downing SR, MacDonald TY, et al. Targeted next-generation sequencing of advanced prostate cancer identifies potential therapeutic targets and disease heterogeneity. Eur Urol 2013;63(5):920–6 doi 10.1016/j.eururo.2012.08.053. [PubMed: 22981675]
35. Robinson D, Van Allen EM, Wu YM, Schultz N, Lonigro RJ, Mosquera JM, et al. Integrative clinical genomics of advanced prostate cancer. Cell 2015;161(5):1215–28 doi 10.1016/j.cell.2015.05.001. [PubMed: 26000489]
36. van Bokhoven A, Varella-Garcia M, Korch C, Johannes WU, Smith EE, Miller HL, et al. Molecular characterization of human prostate carcinoma cell lines. Prostate 2003;57(3):205–25 doi 10.1002/pros.10290. [PubMed: 14518029]
37. Sampson N, Neuwirt H, Puhr M, Klocker H, Eder IE. In vitro model systems to study androgen receptor signaling in prostate cancer. Endocr Relat Cancer 2013;20(2):R49–64 doi 10.1530/ERC-12-0401. [PubMed: 23447570]
38. Davis TA, Loos B, Engelbrecht AM. AHNAK: the giant jack of all trades. Cell Signal 2014;26(12):2683–93 doi 10.1016/j.cellsig.2014.08.017. [PubMed: 25172424]
39. Sekiya F, Bae YS, Jhon DY, Hwang SC, Rhee SG. AHNAK, a protein that binds and activates phospholipase C-gamma1 in the presence of arachidonic acid. J Biol Chem 1999;274(20):13900–7. [PubMed: 10318799]
40. Lee IH, Lim HJ, Yoon S, Seong JK, Bae DS, Rhee SG, et al. Ahnak protein activates protein kinase C (PKC) through dissociation of the PKC-protein phosphatase 2A complex. J Biol Chem 2008;283(10):6312–20 doi 10.1074/jbc.M706878200. [PubMed: 18174170]
41. Shankar J, Messenberg A, Chan J, Underhill TM, Foster LJ, Nabi IR. Pseudopodial actin dynamics control epithelial-mesenchymal transition in metastatic cancer cells. Cancer Res 2010;70(9):3780–90 doi 10.1158/0008-5472.CAN-09-4439. [PubMed: 20388789]
42. Sudo H, Tsuji AB, Sugyo A, Abe M, Hino O, Saga T. AHNAK is highly expressed and plays a key role in cell migration and invasion in mesothelioma. Int J Oncol 2014;44(2):530–8 doi 10.3892/ijo.2013.2183. [PubMed: 24253341]
43. Jung H, Kim JY, Kim KB, Chae YC, Hahn Y, Kim JW, et al. Deacetylase activity-independent transcriptional activation by HDAC2 during TPA-induced HL-60 cell differentiation. PLoS One 2018;13(8):e0202935 doi 10.1371/journal.pone.0202935. [PubMed: 30142192]
44. Sohn M, Shin S, Yoo JY, Goh Y, Lee IH, Bae YS. Ahnak promotes tumor metastasis through transforming growth factor-beta-mediated epithelial-mesenchymal transition. Sci Rep 2018;8(1):14379 doi 10.1038/s41598-018-32796-2. [PubMed: 30258109]
45. Chen B, Wang J, Dai D, Zhou Q, Guo X, Tian Z, et al. AHNAK suppresses tumour proliferation and invasion by targeting multiple pathways in triple-negative breast cancer. J Exp Clin Cancer Res 2017;36(1):65 doi 10.1186/s13046-017-0522-4. [PubMed: 28494797]
46. Zhao Z, Xiao S, Yuan X, Yuan J, Zhang C, Li H, et al. AHNAK as a Prognosis Factor Suppresses the Tumor Progression in Glioma. J Cancer 2017;8(15):2924–32 doi 10.7150/jca.20277. [PubMed: 28928883]
47. Tourinho-Barbosa R, Srougi V, Nunes-Silva I, Baghdadi M, Rembeyo G, Eiffel SS, et al. Biochemical recurrence after radical prostatectomy: what does it mean? Int Braz J Urol 2018;44(1):14–21 doi 10.1590/S1677-5538.IBJU.2016.0656. [PubMed: 29039897]
48. Dai X, Gan W, Li X, Wang S, Zhang W, Huang L, et al. Prostate cancer-associated SPOP mutations confer resistance to BET inhibitors through stabilization of BRD4. Nat Med 2017;23(9):1063–71 doi 10.1038/nm.4378. [PubMed: 28805820]
49. Welti J, Sharp A, Yuan W, Dolling D, Nava Rodrigues D, Figueiredo I, et al. Targeting Bromodomain and Extra-Terminal (BET) Family Proteins in Castration-Resistant Prostate Cancer (CRPC). Clin Cancer Res 2018;24(13):3149–62 doi 10.1158/1078-0432.CCR-17-3571. [PubMed: 29555663]

50. Gao J, Aksoy BA, Dogrusoz U, Dresdner G, Gross B, Sumer SO, et al. Integrative analysis of complex cancer genomics and clinical profiles using the cBioPortal. Sci Signal 2013;6(269):pl1 doi 10.1126/scisignal.2004088. [PubMed: 23550210]

51. Cerami E, Gao J, Dogrusoz U, Gross BE, Sumer SO, Aksoy BA, et al. The cBio cancer genomics portal: an open platform for exploring multidimensional cancer genomics data. Cancer Discov 2012;2(5):401–4 doi 10.1158/2159-8290.CD-12-0095. [PubMed: 22588877]

52. Culig Z, Santer FR. Androgen receptor signaling in prostate cancer. Cancer Metastasis Rev 2014;33(2–3):413–27 doi 10.1007/s10555-013-9474-0. [PubMed: 24384911]

53. Lim HJ, Kang DH, Lim JM, Kang DM, Seong JK, Kang SW, et al. Function of Ahnak protein in aortic smooth muscle cell migration through Rac activation. Cardiovasc Res 2013;97(2):302–10 doi 10.1093/cvr/cvs311. [PubMed: 23042471]

54. Kregel S, Malik R, Asangani IA, Wilder-Romans K, Rajendiran T, Xiao L, et al. Functional and Mechanistic Interrogation of BET Bromodomain Degraders for the Treatment of Metastatic Castration Resistant Prostate Cancer. Clin Cancer Res 2019 doi 10.1158/1078-0432.CCR-18-3776.

55. Xiang Q, Zhang Y, Li J, Xue X, Wang C, Song M, et al. Y08060: A Selective BET Inhibitor for Treatment of Prostate Cancer. ACS Med Chem Lett 2018;9(3):262–7 doi 10.1021/acsmedchemlett.8b00003. [PubMed: 29541371]

56. Hupe MC, Hoda MR, Zengerling F, Perner S, Merseburger AS, Cronauer MV. The BET-inhibitor PFI-1 diminishes AR/AR-V7 signaling in prostate cancer cells. World J Urol 2018 doi 10.1007/s00345-018-2382-8.

57. Gadd MS, Testa A, Lucas X, Chan KH, Chen W, Lamont DJ, et al. Structural basis of PROTAC cooperative recognition for selective protein degradation. Nat Chem Biol 2017;13(5):514–21 doi 10.1038/nchembio.2329. [PubMed: 28288108]

Implications:

BRD4 functions as the dominant regulator of CRPC cell migration and invasion through direct transcriptional regulation of AHNAK, which together offer a novel targetable pathway to treat metastatic CRPC.

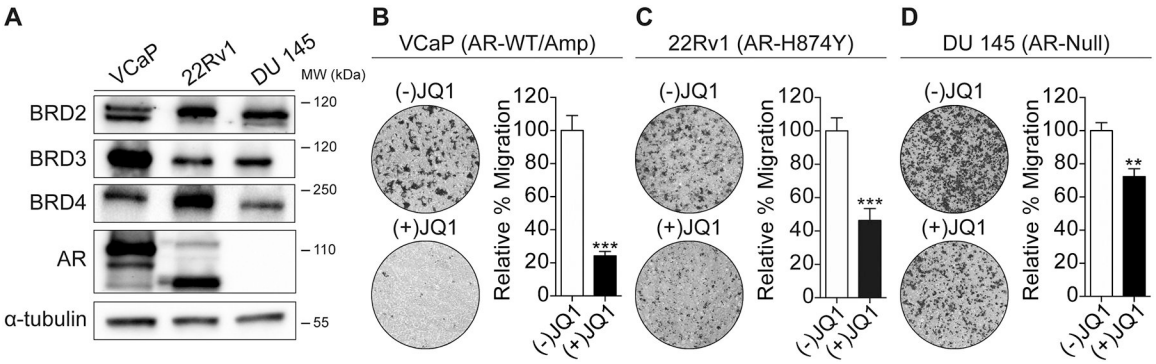

Figure 1. Pan-BET inhibition reduces prostate cancer cell migration in multiple models of CRPC

A, Expression of endogenous BET proteins (BRD2, BRD3, BRD4) and androgen receptor (AR) in three prostate cancer cell lines was detected by immunoblot, compared to α-tubulin. Molecular weights (MW) in kDa corresponding to the immunoblotted proteins are indicated. (**B-D**) VCaP, 22Rv1 and DU 145 cells, respectively, were pre-treated with either 400 nM (+)JQ1, or (−)JQ1 as a negative control, in complete medium (VCaP) or serum-free conditions (22Rv1 and DU 145), for 3 hours. VCaP, 22Rv1 and DU 145 cells were then challenged for migration for 48 hours, 24 hours and 6 hours with undiluted FBS, 10% FBS or 2.5% FBS, respectively, using a transwell system. Results are shown as percentage of cells that migrated, relative to (−)JQ1 control. Left panel: representative images of the total membrane area showing migrated cells stained with crystal violet. Right Panel: Bars represents means ± SEM of three independent experiments. Statistical analyses were performed using the Student's t test. Significant differences between means are defined as: *, $P < 0.05$; ***, $P < 0.001$.

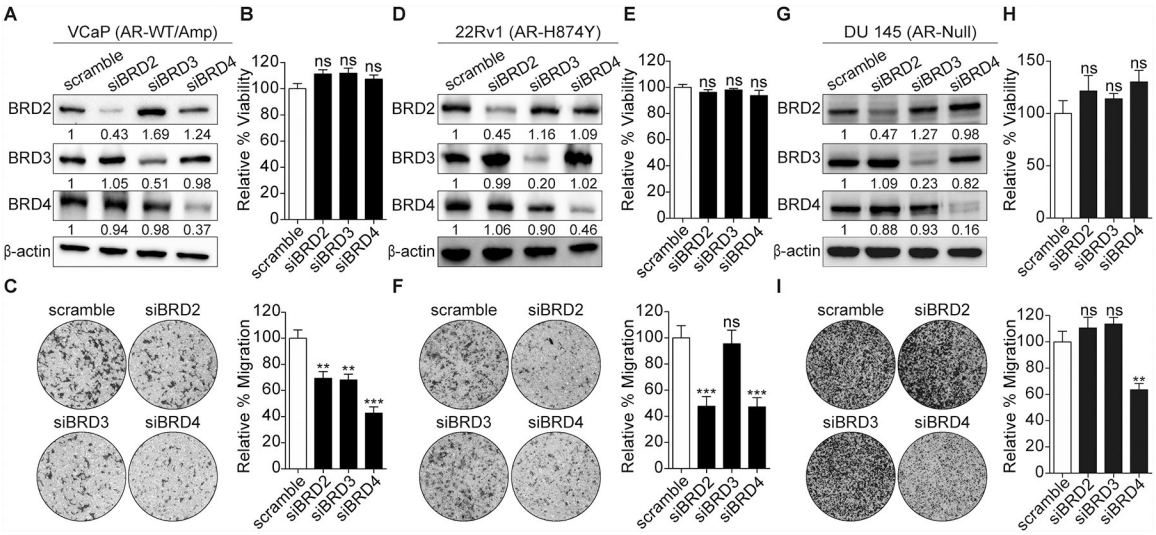

Figure 2. BRD4 regulates CRPC cell migration irrespective of AR status

(**A, D, G**) BET protein-depletion by siRNA was validated by immunoblot of VCaP, 22Rv1 and DU 145 cells, respectively. Cells were transfected with either 25 nM of control (scramble) siRNA or the indicated BET-specific siRNAs for 72 hours. Quantifications relative to scramble are indicated, with normalization to β-actin as a loading control. Blots shown are representative of three independent experiments.

(**B, E, H**) MTT assay showing viability of VCaP, 22Rv1 and DU 145 cells, respectively, transfected with either BET-specific siRNAs or scramble, under the conditions described above. Results are shown as relative percentage of viable cells, compared to control (scramble). Error bars represent means ± SEM of three independent experiments. Statistical analyses were performed using one-way ANOVA.

(**C, F, I**) VCaP, 22Rv1 and DU 145 cells were transfected with either scramble or BET-specific siRNAs, respectively, for 72 hours and then challenged for migration. Results are shown as relative percentage of viable cells, compared to control (scramble). Representative images are shown as a percentage of migrated area in comparison to the total membrane area. Error bars represent means ± SEM of three independent experiments. Statistical analyses were performed using a one-way ANOVA. Significant differences: ns, nonsignificant, $P > 0.05$; *, $P < 0.05$; **, $P < 0.01$; ***, $P < 0.001$.

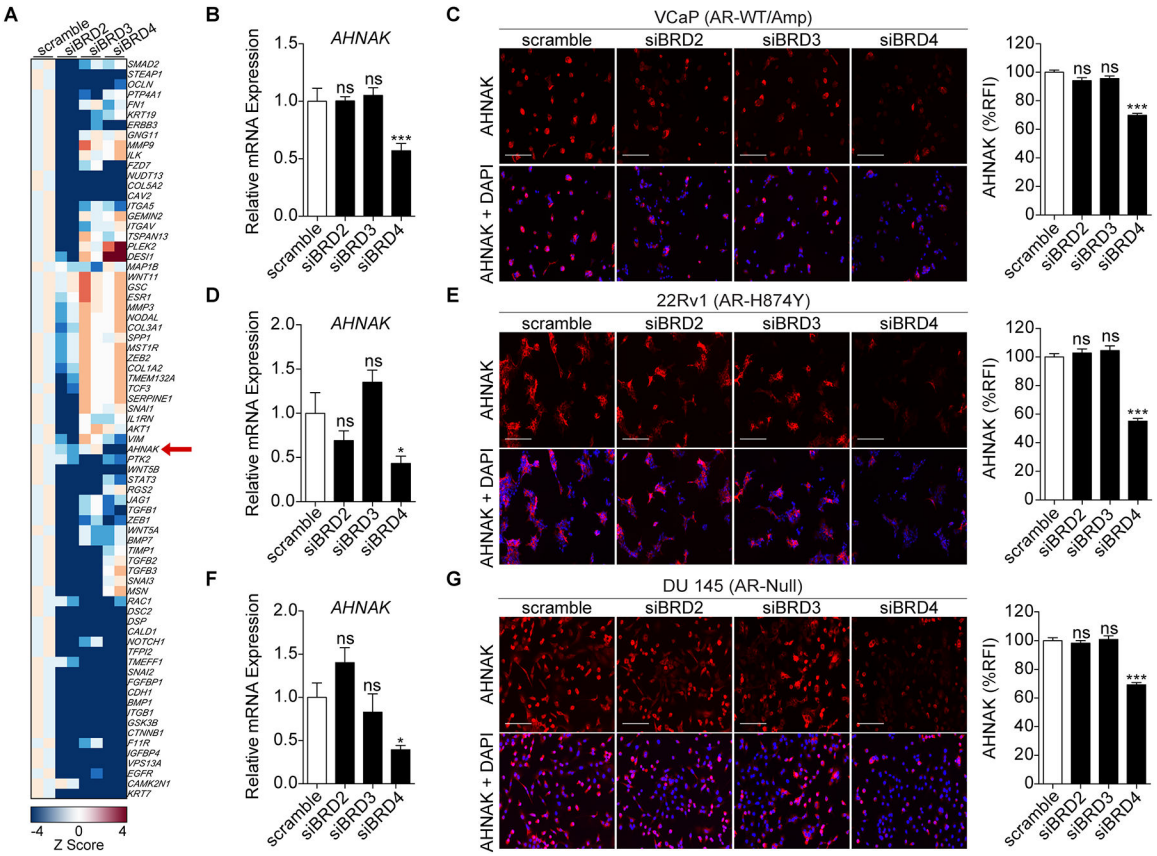

Figure 3. Discovery of *AHNAK* as a BRD4 target gene

A, Heatmap shows the relative expression of 73 genes involved in the regulation of migration, in response to BET protein-depletion in DU 145 cells. Z scores are represented using a blue-to red color code. Results from two independent experiments are shown. AHNAK is indicated (red arrow).

(**B, D, F**) *AHNAK* relative mRNA expression measured in VCaP, 22Rv1 and DU 145 cells, respectively, 72 hours after transfection with the indicated siRNAs (scramble; siBRD2, 25 nM; siBRD3, 25 nM; siBRD4, 25 nM). Error bars represent means ± SEM of three independent experiments. Statistical analyses were performed using one-way ANOVA.

(**C, E, G**) Immunofluorescence images showing the expression of AHNAK in VCaP, 22Rv1 and DU 145 cells, respectively, 72 hours after transfection with the indicated siRNAs (scramble; siBRD2, 25 nM; siBRD3, 25 nM; siBRD4, 25 nM). AHNAK is stained in red and nuclei are stained in blue with DAPI in the merged images (lower panels). Scale bar, 100 μm. Quantification of AHNAK immunofluorescence as a percentage of relative fluorescence intensity (%RFI). Bar represents means ± SEM of individual cells (n ≥ 600 - VCaP; n ≥ 400 – 22Rv1 and n ≥ 800 – DU 145). Results from two independent experiments are shown. Statistical analyses were performed using one-way ANOVA.

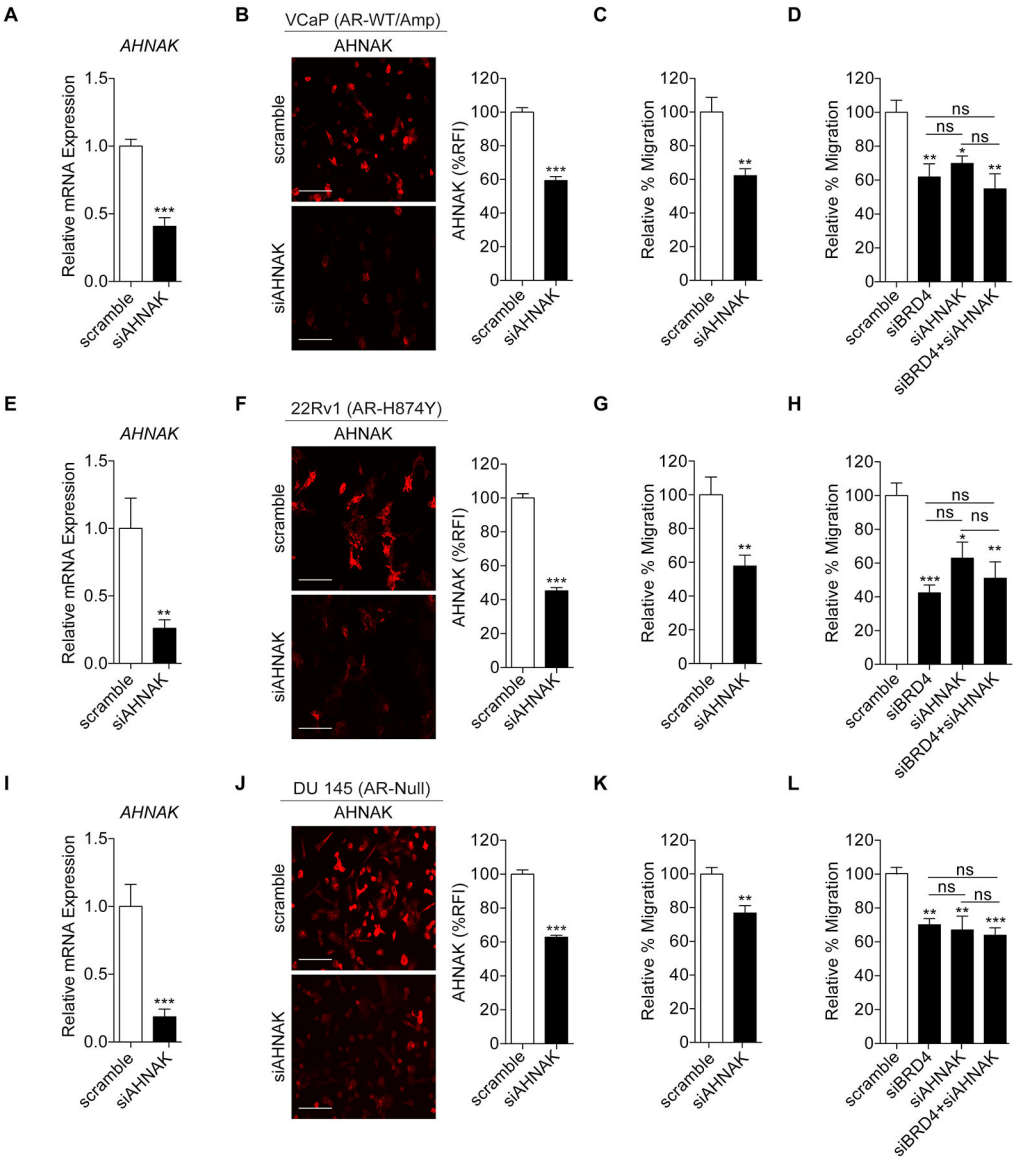

Figure 4. BRD4-AHNAK signaling pathway regulates CRPC cell migration

(**A, E, I**) *AHNAK* relative mRNA expression measured in VCaP, 22Rv1 and DU 145 cells, respectively, 72 hours after transfection with the indicated siRNAs (scramble; siAHNAK, 25 nM). Bar represents means ± SEM of three independent experiments. Statistical analyses were performed using Student's t test.

(**B, F, J**) Immunofluorescence images showing the expression of AHNAK in VCaP, 22Rv1 and DU 145 cells, respectively, 72 hours after transfection with the indicated siRNAs (scramble; siAHNAK, 25 nM). AHNAK is stained in red. Scale bar, 100 μm. Quantification of AHNAK immunofluorescence as a percentage of relative fluorescence intensity (%RFI). Bar represents means ± SEM of individual cells (n ≥ 200 for all models). Results from two independent experiments are shown. Statistical analyses were performed using Student's t test.

(**C, D, G, H, K, L**) VCaP, 22Rv1 and DU 145 cells were transfected respectively with the indicated siRNAs (scramble; siBRD4, and siAHNAK 25 nM or siBRD4 and siAHNAK 25 nM) for 72 hours and then challenged for migration. Results are shown as relative percentage of migration in comparison to control (scramble). Bar represents means ± SEM of three independent experiments. Statistical analyses were performed using Student's t test (F) and one-way ANOVA (G). Significant differences: ns, nonsignificant, $P > 0.05$; *, $P < 0.05$; **, $P < 0.01$; ***, $p < 0.001$).

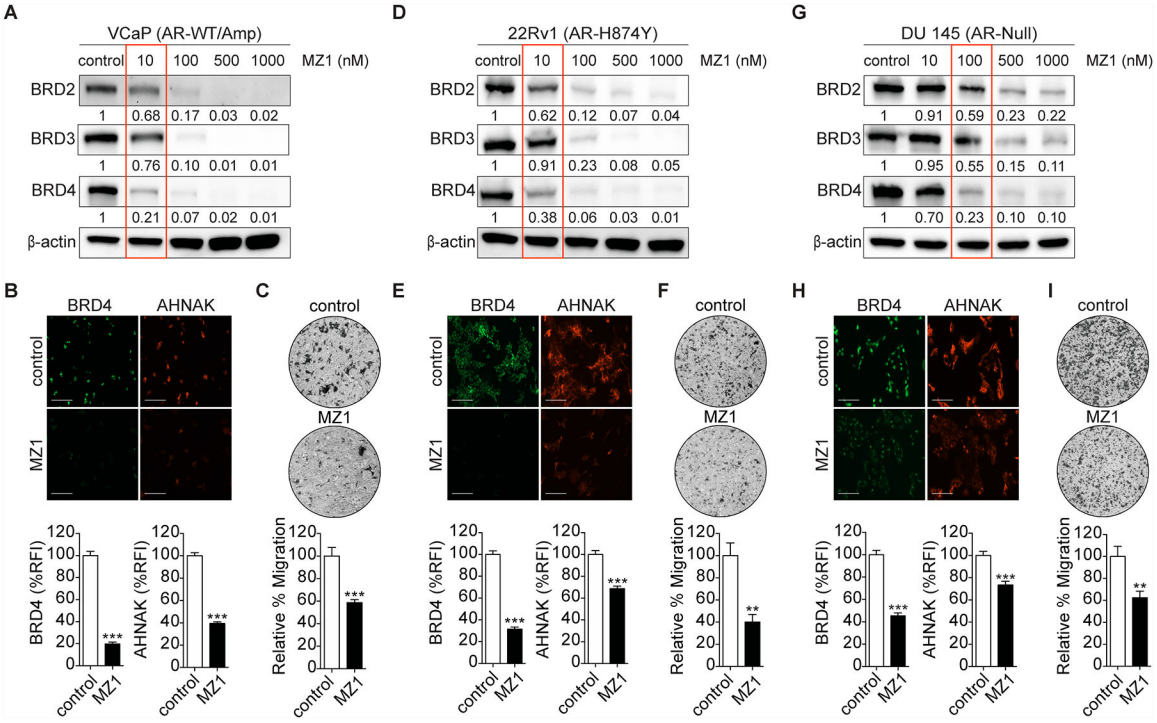

Figure 5. Selective degradation of BRD4 inhibits CRPC migration

(**A, D, G**) Immunoblot of BET protein expression in VCaP, 22Rv1 and DU 145 cells treated with the indicated doses of MZ1 for 24 hours. Quantifications are indicated relative to control (0.01% DMSO); normalization used β-actin as a loading control. Red box indicates optimal dose for selective BRD4 degradation. Blots are representative of two independent experiments.

(**B, E, H**) Immunofluorescence images showing expression of BRD4 and AHNAK in VCaP, 22Rv1 and DU 145 cells after treatment with either 10 nM MZ1 (VCaP and 22Rv1) or 100 nM MZ1 (DU 145) for 24 hours. BRD4 is stained in green and AHNAK is stained in red. Scale bar, 100 μm. Quantification of BRD4 and AHNAK immunofluorescence as a percentage of relative fluorescence intensity (%RFI). Bar represents means ± SEM of individual cells ($n \geq 200$ for all models). Results from two independent experiments are shown. Statistical analyses were performed using Student's t test.

(**C, F, I**) VCaP, 22Rv1 and DU 145 cells, respectively, were pretreated with either 10 nM MZ1 (VCaP and 22Rv1) or 100 nM MZ1 (DU 145) for 21 hours, and then for 3 hours under serum free conditions. Cells were then challenged for migration under conditions described previously using a transwell system. Results are shown as percentage of cells that migrated, relative to control. Left panel: representative images of the total membrane area showing migrated cells stained with crystal violet. Right Panel: Bars represent means ± SEM of three independent experiments. Statistical analyses were performed using Student's t test. Significant differences: *, $P < 0.05$; ***, $p < 0.001$.

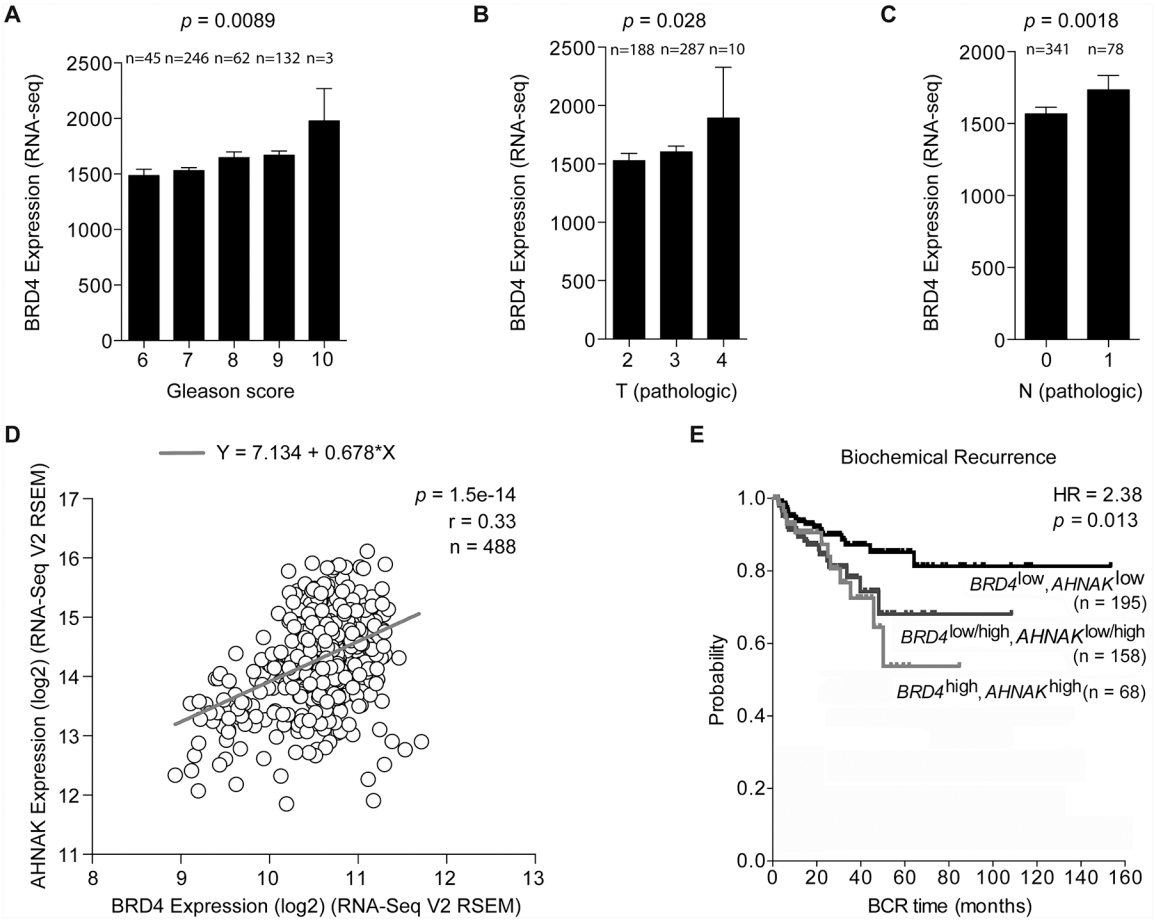

Figure 6. BRD4 and AHNAK expression associate with prostate cancer clinical parameters and biochemical recurrence-free survival

(**A–C**) Correlation between BRD4 expression and Gleason score, pathological T and pathological N. Bar represents means ± SEM (A) or means ± 95% CI (B and C) with number of individuals per parameter indicated.

D, Comparison of BRD4 and AHNAK expression in 488 clinical samples by linear regression. Spearman rank correlation, *p* value and total number of individuals indicated.

E, Kaplan-Meier curve of biochemical recurrence-free survival of 421 prostate cancer patients was calculated from the TCGA database. Patients were segregated into cohorts with 'high expression' (*BRD4*^{high} and *AHNAK*^{high}) and 'low expression' (*BRD4*^{low} and *AHNAK*^{low}) and remaining samples (BRD4$^{low/high}$ and AHNAK$^{low/high}$). Hazard ratio and *p* value are indicated.

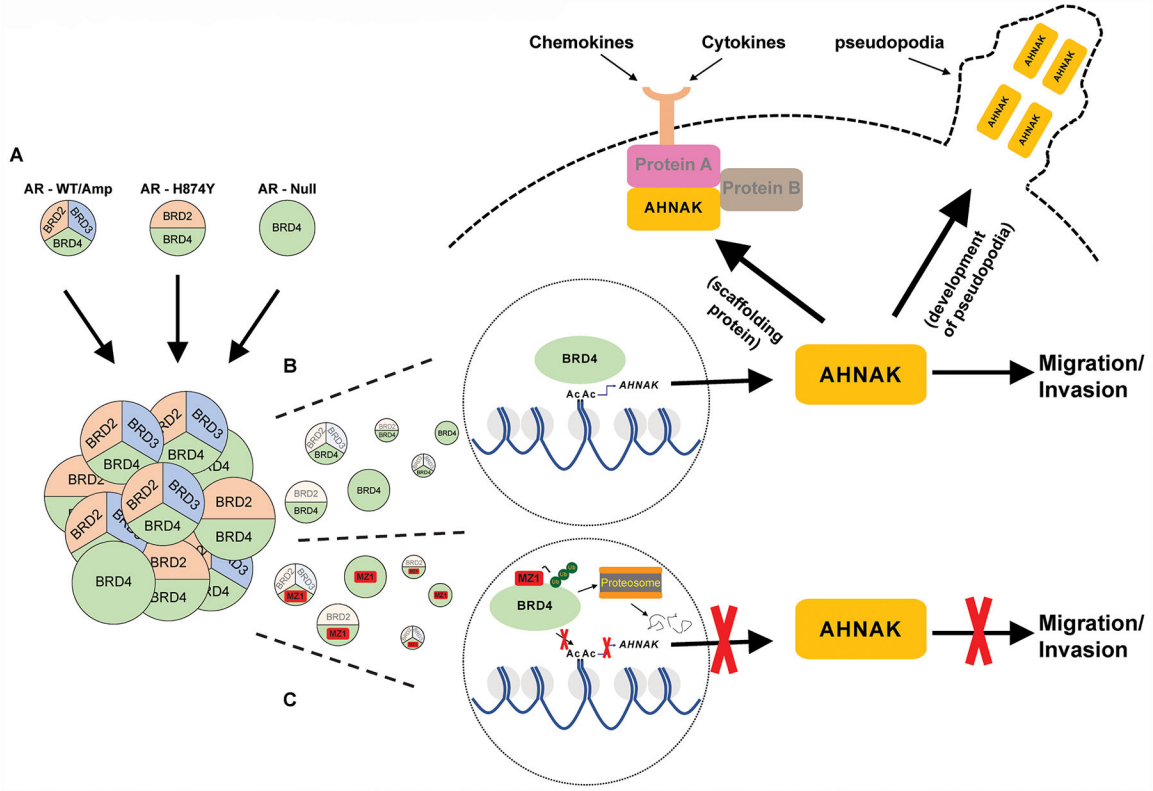

Figure 7. Visual overview of BRD4 regulation of CRPC cell migration and invasion

A, Graphical depiction of different AR status represented in the CRPC cell lines from this study, and the corresponding BET proteins that regulate cell migration. The merging of the three cell types and the numbers that represent each type illustrate the AR heterogeneity that has been previously observed in multiple genomic studies of mCRPC tumors.

B, Graphic highlights BRD4 regulation of AHNAK transcription through BRD4 interaction with the AHNAK promoter, and how within each cell type, only BRD4 is capable of carrying out this process. AHNAK is then shown to facilitate migration and invasion through its ability to develop pseudopodia, while also serving as a scaffolding protein for a variety of canonical signaling pathways that interact with factors secreted from the tumor microenvironment.

C, Illustration showing MZ1 selectively binding to and destroying BRD4 through polyubiquitination and proteasome-dependent degradation. As a result, BRD4 is unable to recruit co-activator proteins to the AHNAK promoter and carry out transcription of AHNAK. Lack of AHNAK represses the migratory and invasive capabilities of the cells. As a result, cell migration and invasion are impaired.